IEICE TRANSACTIONS

on Electronics

DOI:10.1587/transele.2024ECS6002

Publicized:2024/07/17

A PUBLICATION OF THE ELECTRONICS SOCIETY

The Institute of Electronics, Information and Communication Engineers
Kikai-Shinko-Kaikan Bldg., 5-8, Shibakoen 3chome, Minato-ku, TOKYO, 105-0011 JAPAN

BRIEF PAPER

Strong nonlinear effects of a transmission line stub on resonant tunneling diode oscillators

Umer FAROOQ[†], **Masayuki MORI**[†], *Nonmembers*, *and* **Koichi MAEZAWA**[†*a)], *Senior Member*

SUMMARY This study discusses the behavior of resonant tunneling diode (RTD) oscillators when a transmission line (TL) stub is added. The TL stub acts as a delayed feedback unit, resulting in unstable and complex oscillation behavior. Circuit simulation showed that the circuits generate various waveforms, including chaos, by changing the stub length. Experimental demonstration of the simulation results was performed using circuits fabricated with hybrid integration techniques using an InGaAs/AlAs RTD. These complex signals have potential for various applications in the THz frequency range. On the other hand, this finding is significant for the design of THz oscillators using an RTD, since even a small metal pattern can cause such a feedback effect in the THz frequency range. In particular, interconnect wiring patterns can cause this effect because reflection due to impedance mismatch is unavoidable.

key words: *resonant tunneling diode, chaos, microwave frequency, transmission line*

1. Introduction

The resonant tunneling diode (RTD) is a highly promising active device for the THz frequency range [1]–[5]. Its negative differential resistance (NDR) serves as the basis for oscillators, and 1.98 THz oscillation has already been reported using the RTD [6]. Recent studies have also explored the potential of RTD oscillators for ultrahigh-speed wireless communications [7]–[9]. Additionally, RTDs have potential applications in sensors. We have proposed and demonstrated sensors that use RTD oscillators to detect frequency changes due to external parameters [10], [11]. These sensors employ the frequency delta sigma modulation (FDSM) technique, which allows for measuring frequency changes with ultrahigh dynamic range and wide bandwidth [12]–[14]. In any case, the stability of the oscillation frequency in the RTD oscillators is a key factor in achieving high performance [15].

It is important to note that the RTD is a two-terminal device, which has an inherent disadvantage. This can result in frequency fluctuations caused by changes in load impedance and spurious oscillations at the bias node [16]–[18]. In addition, the oscillator behavior is sensitive to the circuit patterns and wiring lines. In this paper, we will demonstrate the complex behaviors, including chaos, that can occur in the RTD oscillators when a transmission line (TL) stub is added. The TL stub can be considered as a delayed feedback unit that introduces a strong nonlinearity into the circuit, leading to chaos [19]–[22]. This mechanism is different from that discussed in our previous papers [23]–[25]. The circuit discussed in the previous papers is a forced van der Pol oscillator and produces complex signals due to the conflict between the external signal frequency and the internal resonance frequency. On the other hand, the present circuit produces complex signals due to the conflict between the oscillation period and the delay time of the reflected signal in the TL stub. In addition to the mechanism, there is an important difference that affects the analysis of the circuit, namely, the present circuit is a self-oscillating circuit and it has no fixed reference frequency to sample the waveform signal. This difference makes the analysis of this circuit more difficult.

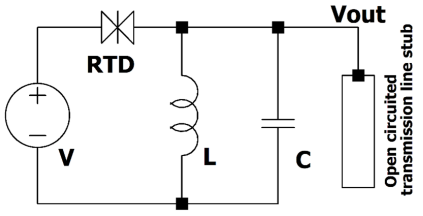

Fig. 1 Basic circuit diagram of RTD-based oscillator along with an open TL stub.

This type of simple and high frequency chaos generator has potential for various applications in the THz frequency range. On the other hand, understanding the effects of such a TL stub is also important for the design of THz circuits using RTDs. This is because even an extremely small stub can produce the nonlinear effects discussed in this paper. For example, a small anomaly in the circuit pattern, such as a stub-like protuberance, can produce such an effect. In addition, a short wiring line for an output or interconnect can produce similar effects due to reflection from an unavoidable impedance mismatch. In short, the importance of nonlinear phenomena increases at higher frequencies.

2. Basic behavior of the RTD oscillator with a TL stub

The circuit being considered here is a free-running RTD oscillator with an open TL stub, as shown in Fig. 1. The oscillator circuit includes an RTD acting as an NDR element, and a parallel connection of an inductor, L, and a capacitor, C, for the resonator. An open stub is connected to the resonator node. This simple stub produces complex behavior

[†]The author is with the Faculty of Engineering, University of Toyama, 3190 Gofuku, Toyama 930-8555, Japan.

[*]Presently, the author is with the Hokuriku Polytechnic College, 1289-1 Kawaberi, Uozu 937-0856, Japan.

a) E-mail: maezawa@ieee.org

in the RTD oscillators via delayed feedback.

First, the effect of the TL stub on the RTD oscillators was investigated by performing the circuit simulation. We used a lossless TL model with 50 Ω characteristic impedance as an open stub, and a Schulman's $I - V$ model [26] with similar characteristics to our RTD fabricated on an InP substrate [27]. This circuit was designed to oscillate at a low GHz frequency to match the experiment described in the next section, although a similar result is expected at much higher frequencies.

A DC bias voltage V_{bias} was applied to bias the RTD in its NDR region, resulting in the initiation of oscillations. The circuit output was then analyzed by varying the length of the open stub. A bifurcation diagram was plotted as a function of stub length in Fig. 2. The stub length was normalized to the wavelength of the fundamental frequency of the circuit without the stub (3.34 GHz). This bifurcation diagram plots the local maxima of the oscillation waveform at the given stub length. This sampling scheme is different from the conventional one, where the sampling is done with the period of the input frequency. We adopted this scheme because it is difficult to define the exact period because this circuit is a free-running oscillator, and the oscillation frequency changes as the TL length changes. In addition, to remove the effects of high-frequency noisy spikes caused by the sharp transition of the RTD current, the output signal was obtained through a low-pass filter (LPF) with the cutoff frequency set to a value slightly higher than the maximum oscillation frequencies. Despite this change, the characteristics of this bifurcation diagram are the same as the conventional one, so that single oscillation gives one point, double period behavior gives two points, and so on. In particular, densely filled regions indicate complex signals, including chaos. This figure demonstrates that the RTD oscillator with an open TL stub shows various complex behaviors. Figure 3 (a) and (b) illustrate an example of the complex waveform and its phase portrait. The phase portrait shows a double scroll attractor, which is considered to be a signature of chaos [28].

It is worth noting that we have also confirmed by simulation that the short-circuited stub has the similar effects as the open stub. The difference is in the reflection phase, and roughly speaking, the short stub with twice the stub length has a similar effect as the open stub. We also note that the phenomena discussed in this paper can take place in the THz oscillators, since the same equivalent circuit well describes the operation of the oscillators in the THz frequency range [29].

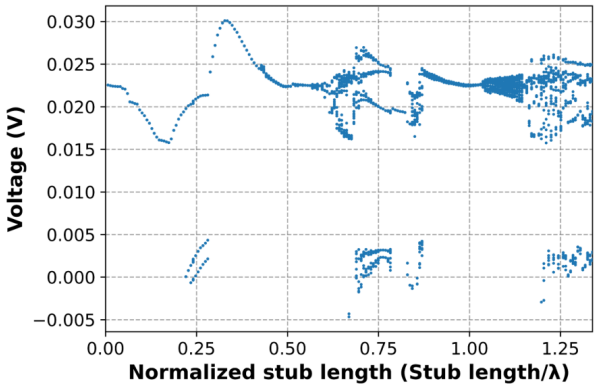

Fig. 2 Simulation result of the bifurcation diagram of the RTD oscillator with an open-circuited stub. The inductance and capacitance used for the resonator were 4 nH and 0.3 pF, respectively.

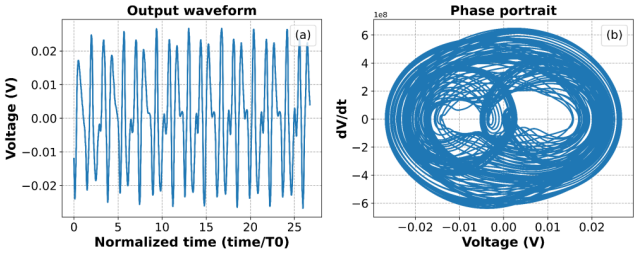

Fig. 3 Chaotic output waveform and double scroll attractor. The normalized stub length is 0.681. L and C are the same as those for Fig. 2.

3. Experiments

3.1 Oscillator fabrication

To confirm the results of the above simulation, we fabricated and tested the RTD oscillator with an open TL stub as shown in Fig. 4. For ease of measurement, the resonant frequency was designed in the low microwave frequency range. The circuit was fabricated using a hybrid integration approach on a 0.8 mm double-sided glass-epoxy FR-4 printed circuit board (PCB) by integrating commercially available 1.0 mm×0.5 mm chip elements and the in-house fabricated RTD chip. The details of the RTD have been described previously [25], [30]. The connection of the RTD to the circuit was facilitated by the bonding wires. Multiple bonding wires were used to reduce their impedance. The oscillation waveforms were observed through the output port, which was coupled to the resonator node via a small capacitor. To avoid spurious oscillations, the bias stabilization resistor of 5 Ω was inserted between the bias node and the ground. The maximum length of the open stub is equal to approximately 1.3 times the wavelength of the fundamental oscillation without the stub.

3.2 Experimental setup

It is difficult to observe complex, non-periodic signals, such as chaos, using a sampling oscilloscope. We employed the experimental technique proposed in our previous paper to characterize the circuit [25]. The experimental setup is illustrated in Fig. 5. The circuit is powered by DC bias voltages in conjunction with the train of pulses. These pulses periodically reset the oscillator and allow the waveform to be observed with a sampling oscilloscope. The output signal was filtered by LPF. This is indispensable because the output signal contains many high frequency components due to the

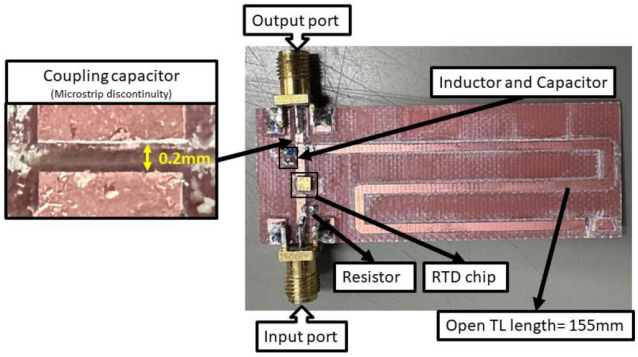

Fig. 4 Prototype circuit to observe the effects of an open stub on the RTD oscillators. The inductance and capacitance used for the resonator were 4 nH and 0.3 pF, respectively. The output port was coupled to the oscillator node via a gap capacitor of approximately 41 fF, as shown in the left figure.

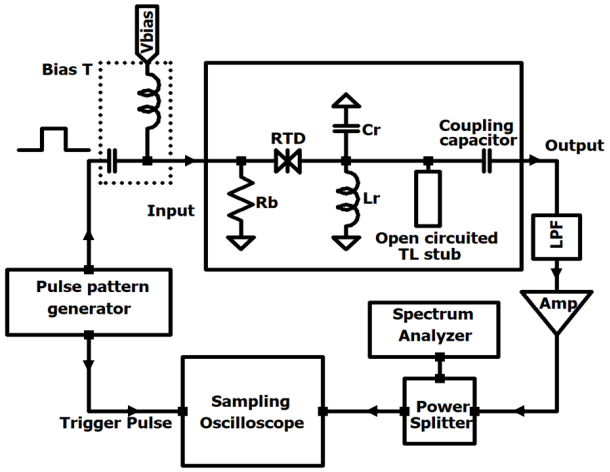

Fig. 5 Experimental configuration for directly observing high frequency non-periodic output signal waveforms.

strong nonlinearity of the RTD. These high frequency components disturb observation of the essential behavior of the oscillator. All instruments were connected to a computer for digital data acquisition.

3.3 Results and discussion

The fabricated circuit without the stub oscillated at about 1.41GHz under DC bias of 1040 mV. To visualize the output waveforms, we injected an 80 MHz pulse accompanied by a DC bias voltages of 880mV. To find the effects of the open stub on the RTD oscillators, the length of the open stub was changed 48 times by sequentially cutting 3mm/5mm length from the open end side using a metal guide cutter. Detailed analysis of the output waveforms was then performed after each cut. By accumulating all the output waveforms acquired from the sampling oscilloscope, the bifurcation diagram was plotted by finding local maxima as shown in Fig. 6. A region of multiple dots indicates complex output, while distinct dots indicate periodic output, which can be single period, double period, and so on.

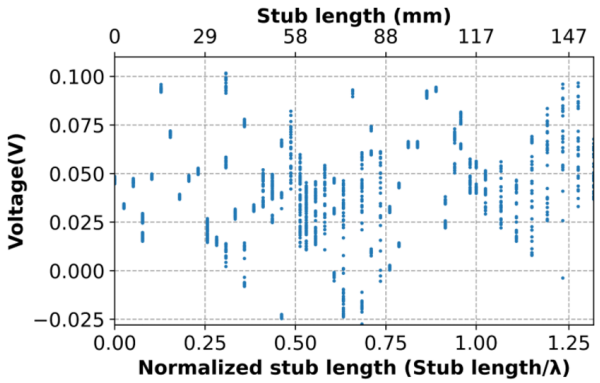

Fig. 6 Experimental bifurcation diagram plotted by varying the open stub length. The stub length is normalized to the wavelength of the oscillation without the stub.

The experimental bifurcation diagram in Fig. 6 looks somewhat different from the simulated one in Fig. 2, however, they have important similarities. First, both bifurcation diagrams consist of complex behaviors unique to nonlinear systems. Next, for normalized stub lengths less than about 0.5, the output is rather simple, consisting of small-period behaviors. Then, for normalized stub lengths greater than 0.5, more complex and non-periodic behaviors appear. In addition, the dense region, which implies chaos or quasi-periodic behavior, seems to appear intermittently as the stub length increases. It should be emphasized that the experimental circuit is affected by many parasitic elements. Such elements should cause large differences in the bifurcation diagram.

Figure 7 shows examples of the experimentally obtained waveforms with their spectrum. Various types of waveforms were observed in this circuit depending on the stub length. The double period behavior is shown in Fig. 7 (a), while the non-periodic signals are shown in Fig. 7 (c) and (e). It should be noted here that the small TL length of 9 mm, which is about 1/13 of the wavelength of the fundamental oscillation frequency, can cause signal modulation.

To further identify the nature of the output waveforms, we reconstructed the phase portrait using the time delay method [31] by taking $V(t)$ on the x-axis and $V(t+\tau)$ on the y-axis. Temporal data were interpolated to smooth the data for clear display of the waveforms and phase portraits. Figure 8 shows phase portraits obtained from the waveforms shown in Fig.7 (c) and (e). Both signals are non-periodic and look random. However, the phase portraits are quite different for each other. The phase portrait for a stub length of 30 mm shows a quasi-periodic attractor, and that for 86 mm shows a very clear double scroll attractor which is considered to be the signature of deterministic chaos [28]. The Lyapunov exponents ($\lambda_{\max}$) were also estimated using the Wolf method [32] for 86 mm, and the largest value obtained was 0.0142. The positive value of $\lambda_{\max}$ is the confirmation of chaos.

Finally, we will briefly discuss the origin of the complex behaviors shown here. As described earlier, these phenomena can probably be explained by the ratio of the delay time to

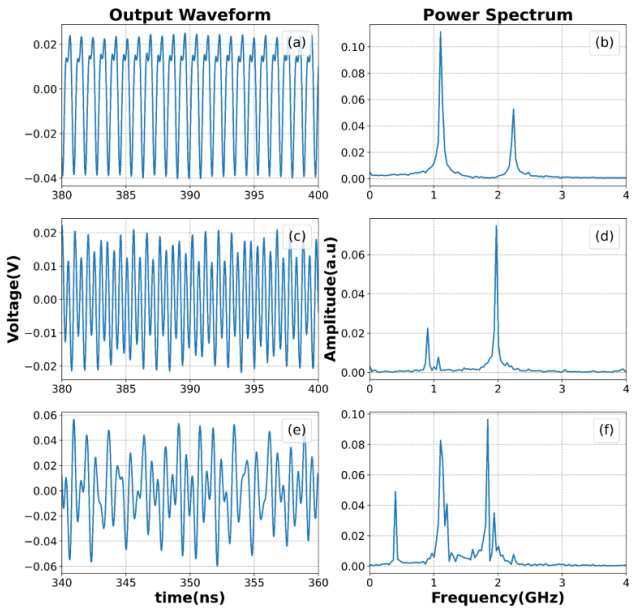

Fig. 7 Examples of experimentally obtained waveforms with their spectrum for various TL lengths. The stub length and its normalized values are (a), (b) 9 mm, 0.0769, (c), (d) 30 mm, 0.256, and (e), (f) 86 mm, 0.735, respectively.

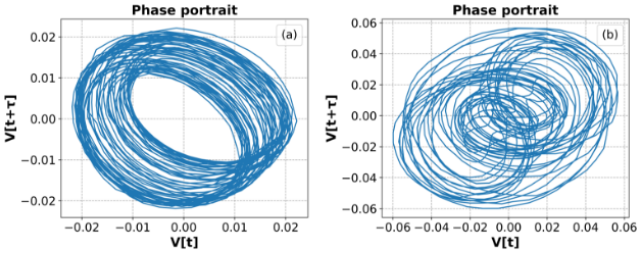

Fig. 8 Phase portraits of the experimentally obtained waveforms. (a) stub length=30 mm, (b) stub length=86 mm.

the period of the oscillation frequency, and their locking and unlocking. The intermittent appearance of the non-periodic region in Fig. 2 and 6 should be a result of this mechanism. However, it is more complicated because the oscillation frequency itself changes depending on the TL length. The detailed discussion is beyond the scope of this paper, and further studies are needed.

4. Conclusion

The behavior of RTD oscillators with an open TL stub was investigated as a function of the stub length. First, a circuit simulation was performed to clarify the basic phenomena caused by the stub. It was found that the open stub induces strong nonlinearities in the RTD oscillators, leading to the evolution of complex behavior, including chaos.

To confirm the simulation results, we fabricated and tested RTD oscillators with an open TL stub. The circuit was fabricated using a hybrid integration technique. The experimental results showed chaotic and periodic output waveforms by varying the open stub length. Consequently, this circuit has potential as a simple chaos generator in the THz frequency range. Moreover, understanding the effects of such a TL stub is also important for the design of THz circuits using RTDs, since even a small metal pattern or interconnection wires can cause such a feedback effect in the THz frequency range.

Acknowledgments

This work was supported by JSPS KAKENHI Grant Number 23K03970, and the VLSI Design and Education Center (VDEC), the University of Tokyo in collaboration with Keysight Technologies Japan, Ltd. A part of this work was carried out under Cooperative Research Project Program of the Research Institute of Electrical Communication, Tohoku University.

References

[1] S. Suzuki, M. Asada, A. Teranishi, H. Sugiyama, and H. Yokoyama, “Fundamental oscillation of resonant tunneling diodes above 1 THz at room temperature,” Appl Phys Lett, vol. 97, no. 24, 242102, 2010.

[2] M. Feiginov, C. Sydlo, O. Cojocari, and P. Meissner, “Resonant-tunnelling-diode oscillators operating at frequencies above 1.1 THz,” Appl Phys Lett, vol.99, no. 23, 233506, 2011.

[3] Y. Koyama, R. Sekiguchi, and T. Ouchi, ”Oscillations up to 1.40 THz from resonant-tunneling-diode-based oscillators with integrated patch antennas,” Applied physics express, vol. 6, no. 6, pp. 064102, 2013.

[4] J. Wang, K. Alharbi, A. Ofiare, H. Zhou, A. Khalid, D. Cumming, and E. Wasige, “High performance resonant tunneling diode oscillators for THz applications,” 2015 IEEE Compound Semiconductor Integrated Circuit Symposium (CSICS), pp.1-4, 2015.

[5] N. Okumura, K. Asakawa, and M. Suhara, “Analysis of Relaxation Oscillation in a Resonant Tunneling Diode Integrated with a Bow-Tie Antenna,” IEICE Transactions on Electronics, vol.E100.C, no. 5, pp. 430-438, 2017.

[6] Asada, M.; Suzuki, S. ”Terahertz Emitter Using Resonant-Tunneling Diode and Applications,” Sensors 2021, 21, 1384, 2021. https://doi.org/10.3390/s21041384

[7] T. Shiode, T. Mukai, M. Kawamura, and T. Nagatsuma, “Giga-bit wireless communication at 300 GHz using resonant tunneling diode detector,” Asia-Pacific Microwave Conference 2011, pp. 1122-1125, 2011.

[8] N. Oshima, K. Hashimoto, S. Suzuki, and M. Asada, “Wireless data transmission of 34 Gbit/s at a 500 - GHz range using resonant - tunnelling - diode terahertz oscillator,” Electron Lett, vol.52, no. 22, pp. 1897-1898, 2016.

[9] N. Oshima, K. Hashimoto, S. Suzuki, and M. Asada, “Terahertz wireless data transmission with frequency and polarization division multiplexing using resonant-tunneling-diode oscillators,” IEEE Trans Terahertz Sci Technol, vol.7, no. 5, pp. 593-598, 2017.

[10] T. Tajika, Y. Kakutani, M. Mori, and K. Maezawa, “Experimental demonstration of strain detection using resonant tunneling delta - sigma modulation sensors,” Physica status solidi (A), vol.214, no. 3, p.1600548, 2017.

[11] K. Maezawa, T. Ito, and M. Mori, “Delta-sigma modulation microphone sensors employing a resonant tunneling diode with a suspended microstrip resonator,” Sensor Review, vol.40, no. 5, pp. 535-542, 2020.

[12] M. Høvin, A. Olsen, T. S. Lande, and C. Toumazou, “Delta-sigma modulators using frequency-modulated intermediate values,” IEEE

J Solid-State Circuits, vol.32, no. 1, pp. 13-22, 1997.

[13] A. Iwata, N. Sakimura, M. Nagata, and T. Morie, "The architecture of delta sigma analog-to-digital converters using a voltage-controlled oscillator as a multibit quantizer," IEEE Transactions on Circuits and Systems II: Analog and Digital Signal Processing, vol.46, no. 7, pp. 941-945, 1999.

[14] S. Li, A. Sanyal, K. Lee, Y. Yoon, X. Tang, Y. Zhong, K. Ragab, and N. Sun, "Advances in Voltage-Controlled-Oscillator-Based ΔΣ ADCs," IEICE Trans. Electron., Vol.E102-C, pp. 509-519, 2019.

[15] K. Maezawa, M. Mori, "Effects of Oscillator Phase Noise on Frequency Delta Sigma Modulators with a High Oversampling Ratio for Sensor Applications," IEICE Trans. Electron., Vol.E104-C, pp. 463-466, 2021.

[16] C. Kidner, I. Mehdi, J. R. East, and G. I. Haddad, "Power and stability limitations of resonant tunneling diodes," IEEE Trans Microw Theory Tech, vol.38, no. 7, pp. 864-872, 1990.

[17] M. Reddy, R. Y. Yu, H. Kroemer, M. J. W. Rodwell, S. C. Martin, R. E. Muller, and R. P. Smith, "Bias stabilization for resonant tunnel diode oscillators," IEEE microwave and guided wave letters, vol.5, no. 7, pp. 219-221, 1995.

[18] K. Maezawa and M. Mori, "Possibilities of large voltage swing hard-type oscillators based on series-connected resonant tunneling diodes," IEICE Transactions on Electronics, vol.101, no. 5, pp. 305-310, 2018.

[19] A. N. Sharkovsky, "Chaos from a time-delayed Chua's circuit," IEEE Transactions on Circuits and Systems I: Fundamental Theory and Applications, vol.40, no. 10, pp.781-783, 1993.

[20] J. N. Blakely and N. J. Corron, "Experimental observation of delay-induced radio frequency chaos in a transmission line oscillator," Chaos: An Interdisciplinary Journal of Nonlinear Science, vol.14, no. 4, pp.1035-1041, 2004.

[21] K. Ozawa, K. Isogai, H. Nakano, and H. Okazaki, "Formal Chaos existing conditions on a transmission line circuit with a piecewise linear resistor," Applied Sciences, vol.11, no. 20, p.9672, 2021.

[22] L. Corti, G. Miano, and L. Verolino, "Bifurcations and chaos in transmission lines," ARCHIV FUER ELEKTROTECHNIK, vol.79, pp. 165-171, 1996.

[23] K. Maezawa, Y. Kawano, Y. Ohno, S. Kishimoto, and T. Mizutani, "Direct observation of high-frequency chaos signals from the resonant tunneling chaos generator," Jpn J Appl Phys, vol.43, no. 8R, p.5235, 2004.

[24] K. Maezawa, Y. Komoto, S. Kishimoto, T. Mizutani, M. Takakusaki, and H. Nakata, "Controlling high-frequency chaos in resonant tunneling chaos generator circuits," IEICE Electronics Express, vol.2, no. 12, pp. 368-372, 2005.

[25] U. Farooq, M. Mori, and K. Maezawa, "Experimental characterization of resonant tunneling chaos generator circuits in microwave frequency range," IEICE Transactions on Electronics, vol.106, no. 5, pp. 174-183, 2023.

[26] J. Schulman, H. De Los Santos, and D. Chow, "Physics-based RTD current-voltage equation," IEEE Electron Device Letters, vol. 17, no. 5, pp. 220-222, 1996.

[27] Y. Ookawa, S. Kishimoto, K. Maezawa, and T. Mizutani, "Novel Resonant Tunneling Diode Oscillator Capable of Large Output Power Operation," IEICE Trans. Electron., vol.E89-C, pp.999-004, 2006.

[28] C. K. Volos, I. M. Kyprianidis, and I. N. Stouboulos, "Experimental study of a nonlinear circuit described by Duffing's equation," 2006.

[29] M. Asada and S. Suzuki, "Room-Temperature Oscillation of Resonant Tunneling Diodes close to 2 THz and Their Functions for Various Applications," J. Infrared Milli Terahz Waves, DOI 10.1007/s10762-016-0321-6, 2016.

[30] K. Maezawa, H. Matsuzaki, M. Yamamoto, and T. Otsuji, "High-speed and low-power operation of a resonant tunneling logic gate MOBILE," IEEE Electron Device Letters, vol.19, no. 3, pp.80-82, 1998.

[31] A. M. Fraser and H. L. Swinney, "Independent coordinates for strange attractors from mutual information," Phys Rev A (Coll Park), vol.33, no. 2, p.1134, 1986.

[32] A. Wolf, J.B. Swift, H.L. Swinney, and J.A. Vastano, "Determining Lyapunov exponents from a time series," Physica D: nonlinear phenomena, vol. 16, no. 3, pp. 285-317, 1985.